

Supplementary Material

Suitability of different methods for measuring black carbon emissions from marine engines

Päivi Aakko-Saksa¹, Niina Kuittinen³, Timo Murtonen¹, Päivi Koponen¹, Minna Aurela², Anssi Järvinen¹, Kimmo Teinilä², Sanna Saarikoski², Luis Barreira², Laura Salo³, Panu Karjalainen³, Ismael K. Ortega⁴, David Delhaye⁴, Kati Lehtoranta¹, Hannu Vesala¹, Pasi Jalava⁵, Topi Rönkkö³, Hilikka Timonen²

Correspondence to: Päivi Aakko-Saksa (paivi.aakko-saksa@vtt.fi)

Contents

S1. BC measuring instruments.....	1
1.1 Smoke meter.....	1
1.2 Photo acoustic method: AVL Micro Soot Sensor (MSS)	3
1.3 Laser Induced Incandescence (LII)	3
1.4 Multiangle Absorption Photometer, MAAP	4
1.5 Aethalometers.....	4
S2. Engines, test set-up and fuels in three test campaigns.....	5
2.1 Campaign A: Laboratory tests with MSD engine.....	5
2.2 Campaign B: On-board campaign description.....	7
2.3 Campaign C: HDS engine in laboratory	9
S3. Support to the results and discussion	9
3.1 Correlations between OC:EC and UV370:BC880 with AAE values	9
3.2 The effect of fuel properties on the BC emissions.....	9
3.3 Campaign A supporting information	10
S4. Particle sizes affect extinction and scattering mass coefficients.....	11
S5. Numerical results.....	11

S1. BC measuring instruments

S1.1 Smoke meter

Characteristics

Smoke meter (SM) measures soot from the raw exhaust gas without the need for exhaust dilution. The results are reported as Filter Smoke Number (FSN) or as black carbon (BC) emissions. Method is based on light absorption. Blackening of filter is measured by the change in optical reflectance of visible light from a loaded filter relative to clean filter (Fig. S2a). SM measurement is a standardized method conforming to ISO 10054 and ISO 8187-3.

Light source/receiver: The relative spectral responsivity of the reflectometer head shall be similar to the luminous efficiency $V(\lambda)$ of the human eye (ISO 10054, definition in CIE 69). The average human eye is most sensitive to light under daylight conditions at a wavelength of 555 nm. ISO 8187-3 defines incandescent light source (2800-3250 K) or a green light-emitting LED having a peak spectral response from 550 to 570 nm, and the same wavelength range is required for the light receiver (photo-electric cell).

Calibration: Most gray value discs available on the market have reflection partly directional and their absorption depends on the wavelength. Hence, standard discs cannot be used for the calibration of different reflectometers. Manufacturer provides disks for calibration. AVL List GmbH presented calibration procedures for the AVL 415SE as follows (Monica Tutuianu, 2019):

- Calibration of the optical reflectometer head with reference reflectance standards (SRS-99-010 reflectance ~ 99 %; SRS-50-010 reflectance ~ 50 %). Calibration is defined in the ISO 10054.

- Linearity check using white standard, and the system switched off the bulb to record the black value (output voltage). For the grey standard, the grey value (output voltage) is recorded and blackening is calculated.
- Calibration of the sampling volume with a standard glass cylinder.

Black carbon concentrations: For reflectometer value of 0, absorption is 100%. In ISO 10054, the filter blackening is relative to the clean filter (Eq. 1). Blackening is equal to FSN, when normalized to the same sampled volume (298 K, 1 bar) corresponding to the effective sampling length of 405 mm.

$$\begin{aligned} \text{FSN} &= (1 - (R_b/R_c)) \times 10 \\ R_b &= \text{reflectometer value of sample} \\ R_c &= \text{reflectometer value of clean filter} \end{aligned} \quad (1)$$

Conversion of FSN to the BC concentration is according to the equation provided by the manufacturer or correlations available also in ISO 8178-1 (2006, eq. A. 16). For AVL415S and AVL 415SE, FSN manufacturer has established FSN correlation to BC empirically (Eq. 2, Fig. S1)(Monica Tutuiianu, 2019). Filter blackening is calculated from the measured reflectometer voltage and calibration. For measurements performed with instruments operated in heated conditions (heated instrument and heated sampling lines):

$$\text{BC} = (\text{FSN} \times 5.32 \times e^{(0.3062 \times \text{FSN})}) / 0.405 \quad (2)$$

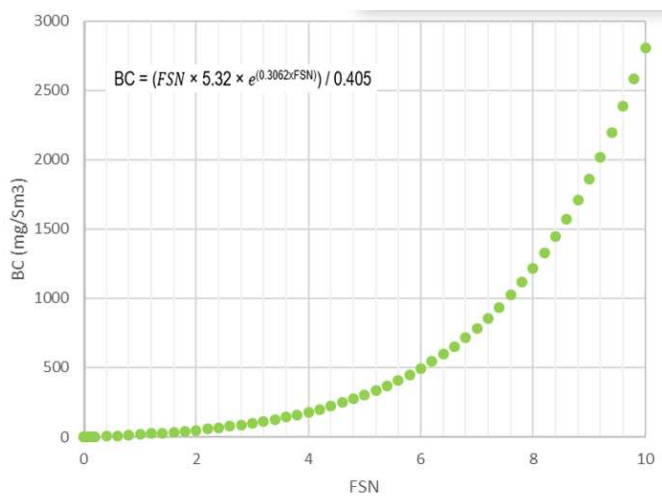


Figure S1. Relationship between BC and FSN as presented in Eq. 3 given by AVL and correlation is also in standard ISO 8178-1.

Mass absorption cross section (MAC) of smoke meter

Authors calculated MAC_{BC} for smoke meters AVL415S and AVL 415SE. In the optical BC instruments the measured light absorption coefficient is converted to BC mass concentration by using mass absorption cross section (MAC) value. MAC (m^2/g) is calculated by dividing the absorption coefficient ($b_{\text{abs}} \text{ m}^{-1}$) attributable to BC by the BC mass concentration (Eq. 3) as described e.g. by Bond et al. (Bond et al., 2013) and Conrad et al. (Conrad and Johnson, 2019).

$$\text{MAC}_{\text{BC}} = b_{\text{abs}} / \text{mBC} \quad (3)$$

Absorption coefficient was calculated from reflectance using the Eq. 4 according to ISO 9835 (Cyrus et al., 2003). In the ISO 10054 measurement, ratio of sample volume (V_s) and effective filter area (A_f) of filter is standardized: $V_s / A_f = 405 \text{ mm}^3/\text{mm}^2$, leading to $A_f/V_s = 2.47 \text{ m}^{-1}$. R_0 is 100% for white filter and R_f (%) is calculated from FSN $((1 - \text{FSN}/10) \times 100$, see Eq. 1). Scale of FSN is from 0 ($R_f = R_0 = 100\%$, white) to 10 ($R_f = 0\%$, black).

$$b_{\text{abs}} = (A_f/V_s)/2 \times \ln(R_0/R_f) \quad (4)$$

MAC_{BC} was derived from Eqs. 1-4. Eq. 2 includes thermophoresis loss, which was taken into account (15% assumed based on MSD engine set-up in laboratory). The results are illustrated in Figure 1 of the main manuscript.

Smoke meters used in the measurements

Two SM instruments were used in these measurements: AVL 415S (owner VTT) and AVL 415SE (Owner AVL List GmbH). The latter model has increased cleaning efficiency and robustness against wet exhaust gas, since shop air purging is introduced. Absolute pressure sensor is also provided.

Range:	0 to 10 FSN or 20 $\mu\text{g m}^{-3}$ to 32 g/m^3 (120 s sampling time even $<10 \mu\text{g m}^{-3}$, note*(AVL List GmbH, 2014))
Resolution:	0.001FSN or 0.01 mg m^{-3}
Detection Limit:	0.002FSN or $\sim 0.02 \text{ mg m}^{-3}$
Exhaust temperature	max. 600 °C with 340 mm probe (800 °C with 780 mm probe)
Compressed air:	appr. 150 L min^{-1} during purge
Sample flow:	appr. 10 L min^{-1}
Sampling time:	from 2 s up to 2 min
Repeatability:	Standard deviation $1 \sigma = \pm (0.005 \text{ FSN} + 3\% \text{ of the measured value})$ at 10 s intake time

*) Measuring low soot concentrations with AVL 415SE and later generation series is possible by increasing the sampling times up to 120 s for measuring low BC concentrations (AVL List GmbH, 2014). Filter blackening with soot concentrations $<10 \text{ mg m}^{-3}$ representing FSN <1 was reported when sampling time increased from 30 s to 120 s. In 1 s, the sampled volume is 50 ml and in 6 s 1000 mL.(AVL List GmbH, 2014)

S1.2 Photo acoustic method: AVL Micro Soot Sensor (MSS)

The measurement principle of the MSS is based on the photo acoustic method, in which a modulated laser beam (heating) causes a sound pressure wave detected by a microphone (Fig. S2b). Diluted exhaust gas is directed through a measuring chamber and thermally animated by a modulated laser beam. The sample gas with "black", i.e. strongly absorbing soot particulates, is exposed to modulated light. The periodical warming and cooling and the resulting expansion and contraction of the carrier gas can be regarded as a sound wave and detected by means of microphones. The 808 nm light is absorbed by the particles. Modulated heating produces periodic pressure pulsation, which is detected by a microphone as an acoustic wave. The signal is amplified in a preamplifier and filtered in a "Lock-In"- amplifier.(Monica Tutuianu, 2019; Schindler et al., 2004)

The MSS consists of a sensor unit and a conditioning unit for dilution, and provides a continuous on-line measurement of BC concentration.

For AVL Micro Soot Sensor (MSS), an empirical calibration procedure is employed. The MSS is calibrated by establishing a mass correlation for a well reproducible aerosol, which has absorption properties of soot produced by internal combustion engine. The calibration aerosol is produced by a CAST propane burner (Combustion Aerosol Standard) and has been analyzed for absorption properties. MSS is calibrated using a CAST aerosol vs. EC(TOA) as reference (Monica Tutuianu, 2019). A modified thermal protocol derived from NIOSH5040 is used for TOA analysis. A gravimetric determination (TX40 filter + microbalance) is used to cross-check the results. The MSS calibration procedure has shown good applicability on Black Carbon from a big variety of combustion engines. The MSS performance has been demonstrated and accepted for aircraft engines. MSS is a standard reference instrument for certification of aircraft engines (SAE E-31 AIR 6241).

AVL MSS used in these measurements was owned by AVL List GmbH.

- Time resolved signal: up to 10Hz
- Rise time $<1 \text{ s}$
- Sensitivity $5 \mu\text{g m}^{-3}$
- Detection limit $1 \mu\text{g m}^{-3}$
- Range $0.001\text{-}50 \text{ mg/m}^3$ (with DR20 up to 1 g m^{-3})
- Dilution ratio 2-20, in these test 7
- Operation temperature $5\text{-}40 \text{ }^\circ\text{C}$
- Sample flow 3.8 L min^{-1}

S1.3 Laser Induced Incandescence (LII)

Laser Induced Incandescence (LII) (ARTIUM 300) measures the thermal emission emitted from soot particles heated by the fundamental mode of a Nd:YAG pulsed laser (usually 1064 nm) to temperatures in the 2500 K to 4500 K range (Fig. S2c). The laser fluence is set to a value which heats the soot particles below their sublimation threshold values (4000 K for black carbon). The emission signal is recorded at an angle of 90° for two specific wavelengths. Emission recorded from LII signals can be used for determinate the mass concentration, volume concentration, active surface area and primary particle diameter of soot particles emissions. LII can measure at a rate of 10 Hz. This is one of the instruments accepted in the aircraft engine certification procedure. ONERA LII is compliant to European Aviation Safety Agency (EASA) requirements for non-volatile Particulate Matter (nvPM) mass concentration measurement.

LII instrument used in these measurements was owned by ONERA.

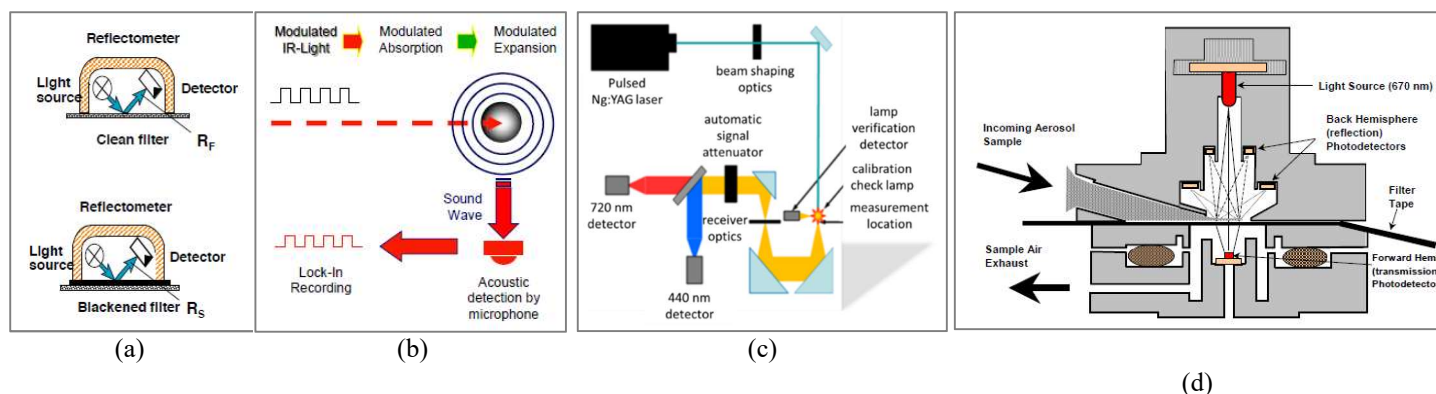


Figure S2. Scheme for a-b) smoke meter and MSS(PAS) (Figures by AVL) c) LII (Figure by manufacturer) d) MAAP (Figure by manufacturer).

S1.4 Multiangle Absorption Photometer, MAAP

MAAP measures the relative change in optical transmission as particles are collected on a filter combined with measurement of reflectance of scattered light with multiple detectors simultaneously (Fig. S2d) (Petzold et al., 2002). Reflection and scattering of light in multiple directions is due to variable particle size and shape. Calculation of BC is based on a specific absorption of BC at a certain wavelength (670nm). MAAP detects transmitted and backscattered light at two angles reducing instrumental artefacts and provides a more accurate measurement of BC than aethalometers. MAAP provides continuous on-line measurement, but requires high dilution ratio for high BC concentrations present in diesel exhaust.

In these measurements, MAAP 5012 manufactured by Thermo Scientific, owned by FMI, was used. Sample flow rates of MAAP were calibrated, and the sample flow rate (6.0 lpm) of MAAP was corrected based on calibration. The results of MAAP were not corrected for spot area, as this correction would have been marginal. Other calibrations of MAAP were not conducted. Hyvärinen et al. (Hyvärinen et al., 2013) developed a semi-empirical correction method for compensating the underestimation of BC by MAAP. In this study, MAAP data was processed with correction algorithm, but this did not affect the results. Therefore additional corrections were not applied. MAAP firmware 1.33 apparently takes into account necessary corrections.

- User-selectable sample averaging times. Automatic temperature and pressure correction.
- PM1 cyclone.
- Filter changes at 20% transmission (appr. 30 μ g) (Glass fiber, GF 10).
- Range: Measurement Range: 0-60, 0-180, μ g m⁻³ BC @ 30, 10, averaging, respectively. (95 % confidence level, 1000 L h⁻¹). In these measurements, 1 min averaging
- Minimum Detection Limits:
 - 2 min. average <100ng m⁻³, <0.66M/m Babs;
 - 10 min. average is <50ng m⁻³, <0.33M/m Babs;
 - 30 min. average is <100ng m⁻³, <0.66M/m Babs

The measurement range of MAAP is narrow. According to the manufacturer, the measurement range of MAAP is 0–60, 0–180, μ g m⁻³ at 30 and 10 min averaging times. However, Hyvärinen et al. (Hyvärinen et al., 2013) reported that MAAP may underestimate BC already at concentrations of 9 μ g m⁻³ at 16.7 L min⁻¹. In this study, flow rate was lower (6 lpm) and averaging time shorter (1 min) than in the cited study.

S1.5 Aethalometers

Aethalometers are based on the change in absorption of transmitted light due to collection of aerosol deposit on reinforced quartz fiber tape, which advances automatically when loading threshold is reached (Hansen et al. 1984). The attenuation of transmitted light is measured continuously. Traditional aethalometers tend to overestimate BC on a fresh filter and underestimate BC on loaded filter. (Arnott et al., 2005) The values measured on lightly loaded filters are deemed to be the closest to the real concentration. (Collaud Coen et al., 2010) A new model MAGEE AE33 is described by Drinovec et al. (Drinovec et al., 2015)

In MAGEE AE42, absorption at 880 nm is interpreted as BC. Additional measurement at 370 nm designated as ‘UVPM’ is interpreted as an indicator of aromatic organic compounds such as are found in tobacco smoke, wood and biomass-burning smoke. Aethalometers can provide continuous on-line BC measurements, but correction of aethalometer data is challenging as corrections should take into account many artefacts and should be applicable to all kind of matrices.

MAGEE AE33 uses seven wavelengths. Measurement of absorption at 880 nm is interpreted as BC. AE33 has also a DUALSPOT™ technology, in which aerosol is collected on two spots in parallel using different loading rates and both spots are simultaneously analysed to avoid "spot loading effects" (Drinovec et al., 2015). Mathematical combination of data yields BC

result independent of "spot loading effects". Simultaneous measurement at multiple wavelengths enables studies of aerosol light absorption, atmospheric optics, radiative transfer, emissions testing, and source apportionment. AE33.

Several coefficients and compensation factors are used in the calculation of the AE33 results (Table S1). Zotter et al.(Zotter et al., 2017) notes that due to the separation of the C value and the MAC, the applied C values should be reported together with determined MAC values. Zotter et al.(Zotter et al., 2017) reported C of 2.14 and $MAC_{BC(880nm)}$ on average $11.8 \text{ m}^2\text{g}^{-1}$ (9.2–15.1 m^2g^{-1}). against EC. These MAC results would correspond to $\sim 9.7\text{--}10.0 \text{ m}^2\text{g}^{-1}$ at 637nm with an absorption Ångström exponent of 0.9–1.0 and a C value of 3.5 instead of 2.14. Deviations from other reported MAC values at similar wavelengths are e.g. $-5\text{--}26 \text{ m}^2\text{g}^{-1}$ due to different methods or differences in BC size and mixing state.

Aethalometers require high DR when BC concentrations are high.

Table S1. Calculation of the results by aethalometer MAGEE 33 as presented in MAGEE manual (MAGEE, 2015).

Optical attenuation:	$ATN = -100 * \ln(I/I_0)$	I_0 =reference signal; I =spot signal
Flow:	$F_{in} = F_{out} * (1 - \zeta)$	F_{out} =measured flow ζ =leakage factor
Attenuation coefficient:	$b_{atn} = \frac{S * (\Delta ATN / 100)}{F_{in} \Delta t}$	S =spot size; t =time
Absorption coefficient:	$b_{abs} = \frac{b_{atn}}{C}$	C =multiple scattering parameter (Weingartner et al. 2003)
Black carbon concentration:	$BC = \frac{b_{abs}}{\sigma_{air}}$	σ_{air} =mass absorption crosssection
Loading effect compensation:	$BC = BC_{measured} / (1 - k * ATN)$	k =compensation parameter
Final equation:	$BC = \frac{S * (\Delta ATN / 100)}{F_{in} (1 - \zeta) * \sigma_{air} * C * (1 - k * ATN_{1}) * \Delta t}$	

In these measurements, MAGEE AE42 is owned by FMI and MAGEE AE33 by Metropolia. Sample flow rates of AE42 were calibrated, but no corrections were needed. The results of aethalometers were not corrected for spot area, as this correction would have been marginal. Other calibrations of aethalometers were not conducted. The BC concentrations for the AE42 were manually selected (representing lightly loaded filters), while the new AE33 defined the BC concentrations automatically. AE-33 used 1 min, 2 L min⁻¹ settings.

AE33:

- Time-base from 1 s or 1 min. Flow rate from 2 to 5 L min⁻¹. Teflon-coated glass fiber filter tape. Tape advances automatically when user selectable loading threshold is reached. PM1 Inlet in use.
- LED Optical Source Range: 370 – 950 nm: (UV), 470 (blue), 520 (green), 590 (yellow), 660 (red), 880 (IR-1) and 950 nm (IR-2). Absorption at 880 nm interpreted as BC and at 370 as UV.
- Resolution: 1 ng m⁻³
- Sensitivity: appr. 0.03 µg m⁻³ (1 min, 5 L min⁻¹)
- Detection limit (1 hour): <0.005 µg m⁻³
- Range: <0.01 to >100 µg m⁻³ BC

AE42:

- Tape advances 1 cm automatically when user selectable loading threshold is reached, time interval depends on BC concentration and flow rate.
- Sensitivity: Proportional to flow rate, inversely proportional to time resolution; approximately 0.1 µg m⁻³ (1 min resolution 3 L min⁻¹ flow rate).

S2 Engines, test set-up and fuels in three test campaigns

S2.1 Campaign A: Laboratory tests with MSD engine

The laboratory MSD measurement campaign A and its test set-up is described earlier as article by Aakko-Saksa et al. (Aakko-Saksa, 2016) as project report (Aakko-Saksa et al., 2017) and here basic features of test campaign are adopted from mentioned publications. The BC results reported have not been used before in comparison with the results of campaigns B and C of this manuscript. New fuel analyses that have not been reported earlier are presented here.

The MSD measurement campaign was carried out with a 1.6 MW Wärtsilä Vasa 4R32 LN medium-speed engine with a modified configuration at VTT's engine laboratory (Table below). Engine test cell is equipped with a versatile fuel handling system for light and heavy fuel oils. Test engine used in this study was equipped with a mechanical injection system.

Table S2. Specifications of the MSD engine in laboratory.

Wärtsilä Vasa 4R32 LN E	
Nominal power, kW	1640
Number of cylinders	4
Speed, rpm	750
Bore/stroke, mm	320/350
Compression ratio	13.8
Rotating direction	Clockwise
Firing order	1-3-4-2
Exhaust valve opens / closes	56 °btdc / 44 °atdc
Inlet valve opens / closes	52 °btdc / 28 °atdc
Injection nozzle opening pressure	520 bar
Static injection advance	12.3 deg

Fuels and lube oil – Tested fuels comprised fuels with 0.1%, 0.5%, 2.5% sulphur contents and a biofuel blend. Marine Diesel Oil with 0.1% sulphur content is abbreviated as “0.1%S”, fuel with 0.5% sulphur content as “0.5%S”, Heavy fuel oil as “2.5%S”, and the blend containing Marine diesel oil and biofuels in ratio of 30:70 as “Bio30”. Fuel and engine oil samples were analysed by ASG Analytik-Service GmbH. Selected fuel properties are shown in Table S3. To meet fuel viscosity requirement of the Wärtsilä Vasa 4R32 engine (about 16 mm²/s), the temperatures of the fuels were adjusted to 28–34 °C for the 0.1%S and the Bio30 fuels, to 100 °C for the 0.5%S fuel and to 134 °C for the 2.5%S fuel. The fuel supply pressures varied from 9.6 to 12 bar. Test cell temperature and humidity stayed relatively constant over the measurement campaign.

Shell Argina XL 40 engine oil was used for the tests. It had been in-use for approximately 200 hours before these tests started. Engine oil analyses showed that engine oil was in good condition both before and after the test campaign. Fresh engine oil showed the lowest metal contents.

Test cycles and set-up - Two engine loads were used, 75% and 25%, corresponding to the open sea and near-harbor engine loading conditions, respectively. A schematic representation of the instrumentation used in the tests is shown in Fig. S3.

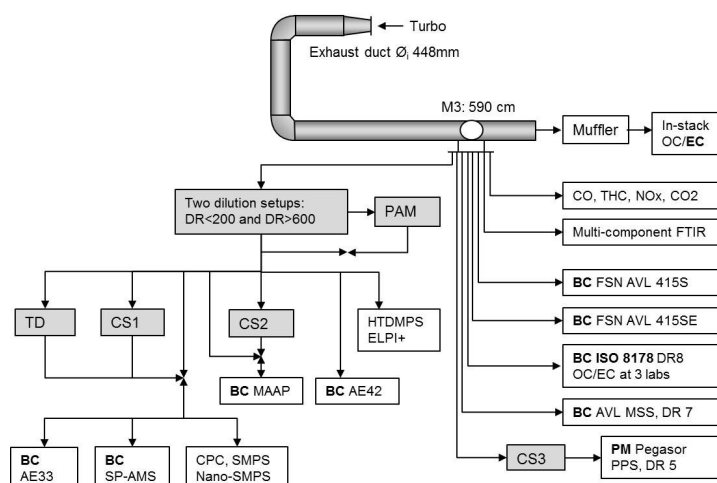


Figure S3. Overview of the instrumentation in the BC measurements in laboratory campaign A (Figure by authors).

Smoke Meter AVL 415S was located below the sampling point, while AVL 415SE was installed above the sampling point. Heated line of 2 m was used for AVL 415S, while heated line of 3 m was used for AVL 415SE, both at 70 °C. Temperature of measuring chamber was 63 °C in both instruments. AVL 415S was remote-controlled and the results were manually recorded. The representative of manufacturer was in charge of the measurements with AVL 415SE, data acquisition and calculations of data. VTT was responsible for the measurements and results obtained with AVL 415S. The Filter Smoke Meter samples raw exhaust without any dilution. In-stack sampling is also conducted from the raw exhaust gas. ISO 8178 PM sampling uses partial flow dilution according to a standardized procedure. AVL Micro Soot Sensor (MSS) used its own diluter.

Aethalometers, MAAP, SP-AMS, particle sizing and Potential Aerosol Mass (PAM) chamber require high dilution ratios (DR). For each fuel, dilution ratio of below 200 was used in standard set-up and higher dilution ratios of 600–1800 were adjusted when PAM was used. Two different high DR setups consisting of several heated and non-heated diluters were used in the measurements. The DR was verified on-line by using gas analyzers at different locations for raw and diluted exhaust gas.

Temperatures, pressures, humidity and dilution air impurities were also monitored. The first DR setup consisted of two-diluters that resulted in a nominal dilution ratio of approximately 100. The primary dilution was executed with a porous tube diluter (PTD) where the dilution ratio was set to about 12. The secondary dilution was executed with an ejector diluter (Dekati diluter) with a nominal dilution ratio of 8. The second DR setup for the measurements where higher DR was necessary, consisted of three diluters: a heated ejector diluter (modified Dekati diluter) with DR of about 4.5 and the temperature of dilution air about 350 °C, secondary dilution with an ejector diluter (Dekati diluter) with a nominal dilution ratio of 8, an adjustable dilution with a mass flow controller and an ejector diluter (Dekati diluter) with a nominal dilution ratio of 8..

Protocol– The 0.1%S fuel was tested at the beginning and at the end of the program to monitor the changes in engine's emissions level over the measurement campaign. Daily protocol included engine warm-up (10 minutes at 50% load and 50 minutes at 75% load); Tests at constant load; Stabilisation of at least 30 minutes between loads.

Catalytic strippers (CS) and thermodenuder (TD)– The effect of sample treatment on measured BC concentration was studied by using catalytic strippers and thermodenuder in front of aethalometers, MAAP, SP-AMS, Scanning Mobility Particle Sizers (Nano-SMPS and Long-SMPS) and Condensation Particle Counter (CPC) according to a pre-defined program. Thermal treatment of the exhaust aerosol removes semivolatile compounds from particles and leaves more solid (or non-volatile) part of particles to be measured, which, in principle, could improve accuracy of BC determination from different exhaust matrices. The CS removes the volatile and semi-volatile organic carbon, and also traps sulphur containing compounds over a catalyst heated to 300 °C. TD removes semivolatile material by adsorption of gaseous compounds. In the TD, the aerosol is first heated to 265 °C, and then the evaporated material is adsorbed by activated carbon. CS1 and TD were periodically on/off before MAGEE AE33. CS2 was periodically on/off before MAAP, and CS3 before PPS-M. For TD, measured solid particle losses were 24.5%, which is in the same range as the losses reported for a CS by Amanitidis et al. (Amanitidis et al., 2018).

S2.2 Campaign B: On-board campaign

The on-board MSD measurement campaign and test set-up is published earlier as project report by (Timonen et al., 2017). The BC results reported have not been used before in comparison with the results of campaigns A and C of this manuscript. Fuel analyses have not been reported earlier.

Measurements of gaseous and particulate emissions of a modern ocean going vessel equipped with scrubber and SCR were conducted during intensive campaign. Fuels during measurements were HFO (0.7% Sulphur) and MGO (<0.1% Sulphur) (Table S3). Measurements were conducted from three points in the vessels exhaust lines for the main engine 1 (ME1) and 2 (ME2);

- Before after treatment for ME2
- Before scrubber ME1 and ME2.
- After the scrubber for ME1 and ME2.

The aims of this measurement campaign were firstly to evaluate suitability of BC instruments for on-board measurements and secondly to conduct in-depth characterization of gaseous and particulate emissions of a modern low emission ship. A special focus was on BC emissions as the international maritime organisation (IMO) limit is anticipated for BC emitted by ships.

Special sampling probes were used for extracting the sample from the exhaust duct. The probes before and after the scrubber were a combination of six separate measurements probes having inner diameter of 6 mm for particulate sampling (five probes) and 4 mm for gaseous components (one probe). Exhaust gas temperature was measured in the both probes. The probe before the scrubber was unheated. Heated lines, heated filters and diluters were connected immediately to the probe outlet and the connections were isolated for avoiding any “cold spots” in the sampling lines. The measurement probe used after the scrubber was heated up to 250 °C to avoid any water droplets to the sampling lines and filters.

FMI and TUT instruments were downstream the PTD dilution system. VTT samplers used their own dilution setups. Several different dilution setups were used. The porous tube diluter (PTD) sampling system for delayed primary aerosols mimics exhaust dilution and nanoparticle formation processes in the atmosphere regarding particle formation by nucleation.(Keskinen and Rönkkö, 2010; Rönkkö et al., 2006) The PTD setup consisted of two diluters that resulted a nominal dilution ratio (DR) of over 100. The primary dilution was executed with a porous tube diluter (PTD) where the dilution ratio was set to be approximately 12, dilution air being at high temperature of 33-39 °C (close to ambient temperature) even though the desired value would be about 30 °C. The secondary dilution was executed with an ejector diluter (ED, Dekati diluter) with a nominal dilution ratio of 8. DRs were verified on-line by using gas analysers at different locations for raw and diluted exhaust gas. Temperature, pressure, humidity and dilution air impurities were also monitored. The third additional diluter, an ED located downstream the PAM chamber, was used during secondary aerosol and reference primary aerosol measurements. The dilution ratios were 168 ± 43 (average \pm st.dev) after the PTD setup and 1050 ± 171 (Average \pm st.dev) after the secondary dilution. In addition the AVL Smart Sampler had its own dilution setup with average DR=10 and DEED sampling was conducted after AVL Smart Sampler (DR=10) and DEEDs own dilution ratio (approx. 800). In addition MSS had its own dilution unit with DR=10.

Altogether more than 20 different instruments were used to characterize the gaseous and particulate emissions. A variety of instruments, MAAP (Multi-angle absorption photometer), Aethalometer (AE33, Magee Scientific, Slovenia), FSN (Filter smoke number, AVL), MSS (Micro Soot Sensor, AVL) were used to measure black carbon (BC) concentrations. In addition, in-depth characterization of gaseous emissions as well as particulate emissions (concentration, composition, size distribution) and their properties (e.g. volatility, secondary aerosol formation potential) of a ship equipped with a modern after treatment system (catalyst

+ scrubber) was achieved by using state-of-the-art online measurement devices; SP-AMS (Aerodyne Research Inc), ELPI (Dekati Oyj), SMPS (TSI), PSM (Airmodus), CPC (TSI), FTIR (Gasmeter DX-4000), Horiba PG-250A, PPS-sensor (Pegasor Oyj), Nephelometer (TSI), Thermodenuder, PAM –chamber (Aerodyne Research Inc) and filter collections (Smart sampler).

Table S3. Properties of the test fuels in MSD engine campaigns.

	LAB-	MSD			On-board	MSD
	0.1%S	0.5%S	2.5%S	Bio30	HFO	MGO
	DMB	IFO	HFO			
Density (15/50 °C), kg/m³	870/-	-/906	-/979	866/-	968/-	873/-
Viscosity (40/50 °C), mm²/s	4.8/-	-/127	-	6.7/-	-/363	3.9/-
Viscosity (80 °C) mm²/s	-	-	187	-		
C, H, % (m/m)					87.7/11.5	87.9/12.8
N, O, % (m/m)					0.25/0.6	-/<0.5
Sulphur content, % (m/m)	0.078	0.375	2.22	<0.0005	0.652	0.078
Hydrogen sulfide, mg/kg	<10	<10	<10	<10		
Water (K.-F.), mg/kg	53	-	-	197		31
Water, % (V/V)	-	0.22	0.54	-	0.2	
Aromatics (mono), % (m/m)	31.8	(28.3)	(22.9)	16.7		26.7
Aromatics (di+), % (m/m)	10.8			2.8		13.0
Asphaltene content, % (m/m)		5.7	28.3		0.36	0.03
Fatty acids/ester, % (V/V)						-/0.1
Total sediment, % (m/m)	<0.01	0.25	0.37	<0.01		
Ash (775 °C) , % (m/m)	<0.005	0.038	0.094	<0.005	<0.005	<0.001
Carbon residue						
10 %D, % (m/m)	<0.1	-	-	2.4		
100 %, % (m/m)	-	3.7	18.3	-	9.6	<0.1
Flash point, °C	86.5	206	103	67.5	146	81
Pour point, °C	0	+30	-5	-9		
Cloud point, °C	+3	-	-	-3		
90 % (V/V) recovery, °C	358	-	-	334		358
Cetane Index/Number	49.9/-	-/44.5	-/26.1	46.4/-		44.3
CCAI	-	780	848	-	828	
Acid number (TAN), mg KOH/g	0.025	0.619	0.776	3.33		
Strong acid number, mg KOH/g	-	-	<0.1	<0.1		
HFRR (lubricity), µm	349	178	154	220		
Copper strip corrosion	1	1	1	1		
Steel corrosion	1	1	intensi- ve rust	1		
Iodine value g I/100g	-	-	-	49		
Heating value, lower kJ/kg	42.5	42.1	40.3	40.7	43.3	44.8
Silver (Ag), mg/kg					<0,5	<0,5
Copper (Cu), mg/kg					<0,5	<0,5
Aluminium (Al), mg/kg					5,7	<0,5
Cadmium (Cd), mg/kg					<0,5	<0,5
Sodium (Na), mg/kg					15,8	<0,5
Potassium (K), mg/kg					<0,5	<0,5
Chromium (Cr), mg/kg					<0,5	<0,5
Manganese (Mn), mg/kg					<0,5	<0,5
Nickel (Ni), mg/kg					12,4	<0,5
Iron (Fe), mg/kg					12,5	<0,5
Molybdenum (Mo), mg/kg					<0,5	<0,5
Barium (Ba) mg/kg					2,0	<0,5
Boron (B) mg/kg					<0,5	<0,5
Calcium (Ca) mg/kg					4,8	<0,5
Magnesium (Mg) mg/kg					0,8	<0,5
Lead (Pb) mg/kg					<0,5	<0,5
Vanadium (V) mg/kg					17,2	<0,5
Tin (Sn) mg/kg					<0,5	<0,5
Zinc (Zn) mg/kg					0,9	<0,5
Silicon (Si) mg/kg					6,0	<0,5
Titanium (Ti) mg/kg					<0,5	<0,5
Phosphorous (P) mg/kg					0,8	<0,5
Cobalt (Co) mg/kg					0,8	<0,5
Lithium (Li) mg/kg					<0,5	<0,5

S2.3 Campaign C: HDS engine in laboratory

Campaign C or its results have not been published before.

HSD engine campaign - VTT's high-speed engine, AGCO 44 AWIC non-road engine in the tests is a modern diesel engine equipped with a common-rail fuel injection system. Test engine represent diesel engines used in heavy-duty vehicles and non-road applications, and also high-speed marine engines for small vessels and boats. Diesel engine was not equipped with exhaust aftertreatment system in these tests.

Table S4. Specifications of the AGCO diesel engine.

AGCO 44 AWIC	
Nominal power, kW	94 @ 2200 min ⁻¹
Nominal torque, Nm	550 @ 1500 min ⁻¹
Number of cylinders	4
Displacement, L	4.4
Compression ratio	16.5
Fuel injection	Common-rail
	Turbocharged, intercooled

Fuels - The following two fuels with different aromatic contents were used in the measurement campaigns with HD diesel engine:

- Diesel fuel meeting EN590 specification, 20 wt% total aromatics (Ar-20)
- Diesel fuel containing 0.1 wt% total aromatics (Ar-0)

Test cycles - Diesel engine was operated according to ISO 8178 RMC-C1 test cycle (developed for Non-road machinery and industrial equipment) with varying engine load modes and durations. In Autumn 2020 cycle was repeated twice resulting in a 3600 s test cycle. In RMC-C1, varying durations of load modes are according to weighing factors of emission standard to reflect typical loads in real operation of heavy-duty engines.

In standardised emission testing, Pallflex TX40 filters were used for PM sampling. TOA analysis of PM was carried out from samples collected on quartz filters.

S3 Support to the results and discussion

S3.1 Correlations between OC:EC and aethalometer UV:BC ($AAE_{370/880}$)

To support discussion in the manuscript, additional ratios of OC:EC and UV:BC channels are presented in Fig. S4. In the manuscript, $AAE_{470/950}$ is presented based on the results obtained by AE33. Here additional information is given on $AAE_{370/880}$ values obtained by AE42 and AE33 instruments.

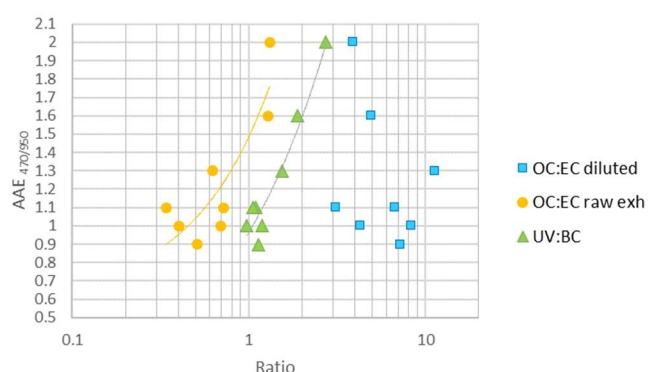


Figure S4. Correlations between OC:EC and UV370:BC880 with AAE values, laboratory MSD campaign.

S3.2 The effect of fuel properties on the BC emissions

Additional information on the relationship between fuel properties and BC emissions is given concerning PAH(di+), asphaltenes and cloud point of fuels. After earlier fuel property analyses (Aakko-Saksa et al., 2016), now also PAH(di+) and asphaltenes were analysed from fuels. Correlations between EC and PAH(di+) and asphaltene contents of fuels were observed at high engine load

(Figure S5a). Assumedly the combustion temperature at high load is sufficient for appropriate combustion to achieve as low EC emissions as specific for fuels. At low engine load, assumedly the combustion is less efficient and hence EC emissions higher than at high engine load. In residual 2.5%S fuel, a known combustion catalyst, Vanadium, was present and may explain its low EC emissions. However, EC concentrations at low engine load correlated surprisingly well with pour point of fuel (Fig. S5b). This may indicate that some fuel constituents having poor cold flow properties have also poor combustion behaviour in this MSD engine at low engine load potentially explaining the high EC emission for 0.5%S fuel at low engine load.

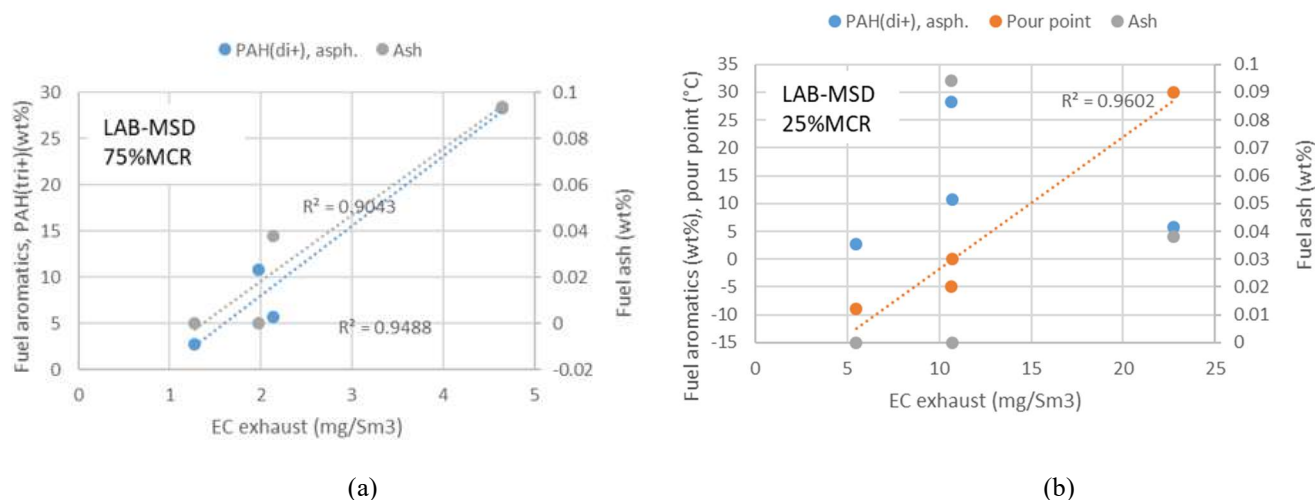


Figure S5. Correlations between fuel properties and EC concentrations in exhaust for the LAB-MSD engine with a) 75% and b) 25% engine loads. The fuel aromatic content and pour point shown in left axis and fuel ash content (wt%) in right axis.

S3.3 Campaign A supporting information

With courtesy of CIMAC, a short summary of selected numerical emission results from campaign A is presented here from Aakko-Saksa et al. (Aakko-Saksa et al., 2016) to support manuscript. PM emission was strongly dependent on the fuel sulphur content. The highest PM emissions were observed for the 2.5%S fuel: 153 mg/Nm³ (850 mg/kWh) at 75% load and 134 mg/Nm³ (1040 mg/kWh) at 25% load. For the other fuels studied, PM emissions varied from 18 to 44 mg/Nm³ (100–240 mg/kWh) at 75% load, and from 52 to 103 mg/Nm³ (390–810 mg/kWh) at 25% load. The BC emission was substantially higher at 25% load than at 75% load. The 2.5%S fuel showed the highest BC emission at 75% load, whereas its BC emission was relatively low at 25% load. The BC emission was dependent on both engine load and fuel properties, but not directly on the sulphur content of fuel. Certain metal oxides present in the 2.5%S fuel may catalytically enhance combustion of BC at 25% load. The 0.5%S fuel showed the highest BC emission at 25% load, which indicates that even at 0.5% sulphur level, the fuel may contain substantial amount of BC precursors depending on crude oil and processing technology. The higher combustion temperature enables more complete combustion of the heavy organic compounds and overrules the effect of metal oxides. The BC emissions for the 0.1%S and Bio30 fuels were substantially lower than those for the 2.5%S at 75% load and for the 0.5%S fuel at 25% load. The lowest BC emission was observed for the Bio30 fuel presumably basing on its oxygen content. Heavy PM PAHs were found at higher concentration for the 0.5%S fuel than for the other fuels. Sum of 10 of the heaviest PAHs¹ analyzed for 0.5%S fuel were 67/151 µg/kWh (75%/25% load), 38/109 µg/kWh and 33/58 µg/kWh for the 2.5%S and 0.1%S fuels, and only 18/45 µg/kWh for the Bio30 fuel. The results indicate that even at 0.5%S level fuel may contain substantial amount of PM PAH precursors depending on crude oil and processing technology.

¹ Benz(a)anthracene, chrysene, benzo(b)fluoranthene, benzo(k)fluoranthene, benzo(e)pyrene, benzo(a)pyrene, perylene, indeno(1,2,3-cd)pyrene, dibenz(a,h)anthracene, benzo(ghi)perylene.

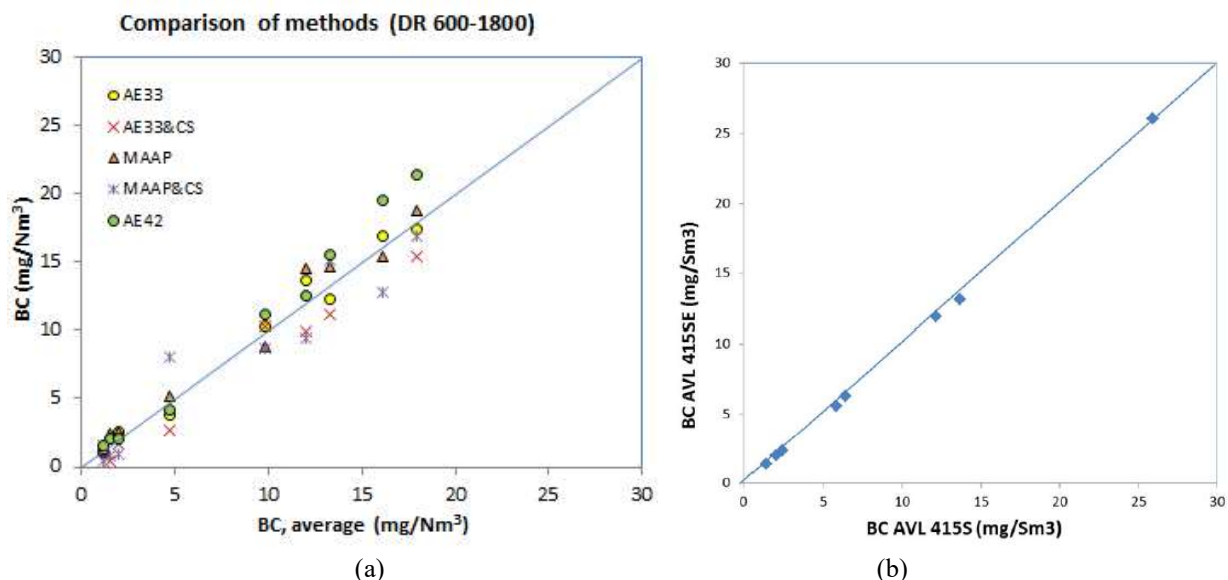


Figure S6. Instruments in the same dilution line (DR 600–1800, aged particles) and correlation between two SM instruments, laboratory measurements with MSD engine. With courtesy of CIMAC (Aakko-Saksa et al., 2016).

S4. Particle sizes affect extinction and scattering mass coefficients

Particle size distribution affects the extinction and scattering mass coefficients as presented by Schindler & Singer in Fig. S7. The mass extinction coefficient of soot² is nearly constant for particle size below 100 nm, while it changes for larger particle sizes.

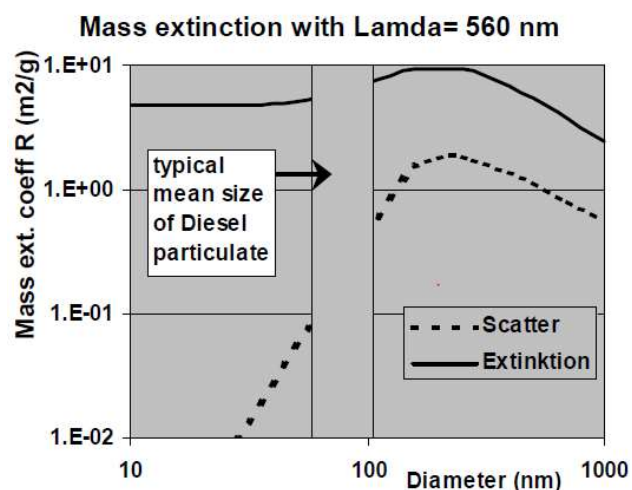


Figure S7. Particle size distribution affect the extinction and scattering mass coefficients (Schindler and Singer, n.d.).

S5. Numerical results

The numerical emission results for WD32 and on-board measurements are shown in units of mass/Sm³, mass per kg oil equivalent (kg_{oe}) or kg fuel and as mass/kWh. Emission per oil equivalent mass (per kg_{oe}) is a commensurable unit, which compensates the differences in the energy contents of fuels. Energy contents of 2.5%S and Bio30 fuels were lower than those of the 0.1%S and 0.5%S fuels mainly due to low hydrogen to carbon ratio of 2.5%S fuel and oxygen content of Bio30 fuel. The concentrations at the prevailing pressure and temperature are normalized to 101 325 Pa and of 273.15 K (Nm³).

For WD32 and AGCO engines, gaseous emissions were typical for diesel engines without aftertreatment devices. For AGCO engine, NO_x emission was 6.6 g/kWh, CO emission 0.34 g/kWh and CO₂ emission was 703 h/kWh. For WD32 engine, HC and CO emissions were lower at 75% load than at 25% load, whereas opposite was seen for the NO_x emission. Combustion temperature

² Soot here is a proxy for a combustion product, black carbonaceous particles, when using hydrocarbon containing fuels in internal combustion engines. Soot has a combustion temperature of over 450 °C in air. It is not volatile or liquid. Schindler&Singer.

typically increases at higher load leading to improved combustion, and consequently higher NO_x emissions. Fuel properties affect emissions, as well, for example oxygen of biofuel tends to increase NO_x emissions (McGill et al., 2003).

Table S5. MSD engine in laboratory, Campaign A. Gaseous emissions, PM and its composition, BC (FSN-based), metals and PAHs.

		75% load					25% load				
		0.1 %S	0.5%S	2.5%S	Bio30	0.1%S	0.1 %S	0.5%S	2.5%S	Bio30	0.1%S
		31.8	4.9	10.9	15.9	21.9	2.9	7.9	11.9	16.9	22.9
NO _x	g/kWh	10,8	11,1	10,9	11,3	11,2	9,2	8,5	8,9	9,5	9,6
HC	g/kWh	0,52	0,31	0,38	0,46	0,48	1,37	0,81	0,87	1,04	1,22
CO	g/kWh	0,33	0,46	0,66	0,30	0,31	1,01	1,49	1,89	0,93	1,02
CO ₂	g/kWh	643	650	686	633	641	750	766	798	730	739
PM ISO8178 (DR=8)	g/kWh	0,11	0,24	0,85	0,10	0,11	0,47	0,81	1,03	0,39	0,50
PM In-stack EN 13284	g/kWh	0,05	0,09	0,56	0,04	0,05	0,20	0,44	1,04	0,11	0,19
BC (FSN)	g/kWh	0,012	0,013	0,032	0,008	0,010	0,098	0,204	0,104	0,048	0,089
Fuel consumption	kg/kWh	0,201	0,203	0,216	0,207	0,200	0,234	0,240	0,252	0,239	0,231
NO _x	g/kg _{oe} fuel	53,1	54,2	52,3	56,0	55,0	38,7	35,3	36,7	40,8	41,0
HC	g/kg _{oe} fuel	2,6	1,5	1,8	2,3	2,4	5,7	3,4	3,6	4,5	5,2
CO	g/kg _{oe} fuel	1,6	2,3	3,2	1,5	1,5	4,2	6,2	7,8	4,0	4,4
CO ₂	kg/kg _{oe} fuel	3,15	3,18	3,30	3,14	3,15	3,15	3,18	3,30	3,14	3,15
PM ISO8178 (DR=8)	g/kg _{oe} fuel	0,54	1,17	4,10	0,48	0,56	1,99	3,35	4,24	1,70	2,13
PM In-stack EN 13284	g/kg _{oe} fuel	0,26	0,43	2,71	0,19	0,26	0,84	1,84	4,30	0,49	0,83
BC (FSN)	g/kg _{oe} fuel	0,056	0,065	0,155	0,037	0,050	0,411	0,847	0,430	0,208	0,380
NO _x	g/Nm3 (wet)	2,0	2,0	1,9	2,1	2,0	1,2	1,1	1,2	1,3	1,3
HC	g/Nm3 (wet)	0,10	0,06	0,07	0,08	0,09	0,18	0,10	0,11	0,14	0,16
CO	g/Nm3 (wet)	0,06	0,08	0,12	0,06	0,06	0,13	0,19	0,25	0,12	0,13
CO ₂	g/Nm3 (wet)	118	118	123	118	117	98	97	104	97	97
PM ISO8178 (DR=8)	mg/Nm3 (wet)	20	44	153	18	21	62	103	134	52	65
PM In-stack EN 13284	mg/Nm3 (wet)	9,7	16,0	101	7,0	9,5	26,0	56,5	136	15,0	25,5
BC (FSN)	mg/Nm3 (wet)	2,1	2,4	5,8	1,4	1,9	12,7	25,9	13,6	6,4	11,6
Fuel consumption	g/Nm3 (wet)	36,9	37,0	38,8	38,5	36,6	30,5	30,5	32,9	31,8	30,2

Average in PM	75% load					25% load					Detection limit µg/Sm3
	0.1%S µg/Sm3	0.1%S µg/Sm3	0.5%S µg/Sm3	2.5%S µg/Sm3	Bio30 µg/Sm3	0.1%S µg/Sm3	0.1%S µg/Sm3	0.5%S µg/Sm3	2.5%S µg/Sm3	Bio30 µg/Sm3	
Ag	2.7	0.1	1.9	0.2	2.7	4.6	0.0	2.1	4.7	1.1	ns
Al	0.0	0.0	132.6	0.0	244.7	0.0	0.0	0.0	0.0	0.0	ns
As	0.5	0.6	1.1	1.1	0.6	1.5	1.0	2.9	3.2	1.6	ns
B	0.0	0.0	0.0	0.0	0.0	0.0	16.1	0.0	0.0	0.0	ns
Ba	0.0	0.0	0.0	0.0	0.0	0.0	31.9	0.0	0.0	0.0	ns
Be	0.1	0.0	0.0	0.0	0.0	0.0	0.0	0.0	0.0	0.4	ns
Bi	16.6	0.1	0.2	0.1	1.1	4.4	0.3	2.6	0.9	1.2	ns
Br	22	61	12	5	6	92	21	28	62	13	
Ca	465	293	345	499	199	620	415	699	963	388	
Cd	bd	bd	bd	bd	bd	bd	bd	bd	bd	bd	<25
Cl	bd	bd	bd	bd	bd	bd	bd	bd	bd	bd	<20000
Co	bd	bd	16	10	bd	bd	bd	bd	8	bd	
Cr	6.1	bd	bd	5.5	bd	12.6	bd	bd	22.1	bd	
Cu	bd	bd	bd	bd	bd	bd	bd	bd	bd	bd	<490
Fe	52	1	145	254	26	57	59	61	147	44	
K	0.0	0.0	0.0	0.0	0.0	0.0	21.3	0.0	0.0	0.0	ns
Li	0.4	bd	bd	bd	bd	0.4	bd	bd	bd	bd	ns
Mg	16	8	12	81	0	9	10	49	47	10	
Mn	3	0	2	9	0	6	2	3	9	2	
Mo	37	38	25	0	0	64	31	100	0	52	
Na	34	7	137	416	0	5	55	233	102	109	
Ni	0	0	139	1714	4	0	3	99	1400	0	
P	25	11	23	18	22	54	37	105	58	49	
Pb	0.4	0.1	1.7	18.7	0.4	0.6	1.2	3.0	22.1	1.7	
Rb	0.0	0.0	0.0	0.0	0.0	0.0	0.2	0.0	0.0	0.0	ns
Sb	bd	bd	bd	bd	bd	bd	bd	bd	bd	bd	<80
Se	0.3	bd	0.8	1.3	0.2	0.6	bd	1.0	1.2	1.0	ns
Si	bd	bd	bd	bd	bd	bd	bd	bd	bd	bd	<500000
Sr	0.0	0.0	0.7	10.4	0.0	0.0	1.0	0.0	5.8	0.0	
Th	0.0	0.1	0.0	0.3	0.0	0.0	0.4	0.6	0.3	0.1	ns
Tl	0.4	bd	bd	bd	bd	0.5	bd	bd	bd	1.2	ns
U	0.0	0.1	0.0	0.0	0.0	0.0	0.4	0.0	0.0	0.0	ns
V	4	10	61	5901	27	bd	10	49	8083	22	
Zn	0.0	0.0	0.0	0.0	0.0	0.0	51.4	0.0	0.0	0.0	ns
Sum	685.5	431.1	1056.4	8945.1	534.3	930.9	767.7	1438.0	10937.6	696.7	

PAHs in PM	75% load				
	0.1%S	0.1%S	0.5%S	2.5%S	Bio30
	µg/Sm3	µg/Sm3	µg/Sm3	µg/Sm3	µg/Sm3
naphthalene*	0.004	0.032	0.018	0.000	0.000
2-methylnaphthalene	0.005	0.017	0.013	0.004	0.002
1-methylnaphthalene	0.006	0.012	0.006	0.000	0.000
biphenyl	0.014	0.071	0.078	0.000	0.012
2,6-dimethylnaphthalene	0.009	0.017	0.010	0.018	0.010
acenaphthylene*	0.000	0.000	0.000	0.000	0.000
acenaphthene*	0.000	0.000	0.000	0.000	0.000
2,3,5-trimethylnaphthalene	0.039	0.077	0.030	0.110	0.034
fluorene*	0.072	0.391	0.509	0.038	0.076
phenanthrene*	0.751	1.372	0.464	1.078	0.272
anthracene*	0.088	0.222	0.088	0.167	0.029
1-methylphenanthrene	1.258	2.182	1.054	1.508	0.365
fluoranthene*	0.490	0.929	0.823	0.740	0.213
pyrene*	3.013	3.494	3.005	0.611	0.639
benz(a)anthracene*	2.251	1.898	2.783	0.623	0.760
chrysene*	3.048	3.546	5.264	4.026	1.735
benzo(b)fluoranthene*	0.744	0.835	1.258	0.629	0.340
benzo(k)fluoranthene*	0.536	0.628	0.876	0.350	0.366
benzo(e)pyrene	0.454	0.495	1.399	0.330	0.241
benzo(a)pyrene*	0.090	0.059	0.256	0.065	0.021
perylene	0.000	0.000	0.000	0.006	0.000
indeno(1,2,3-cd)pyrene*	0.032	0.037	0.165	0.041	0.016
dibenz(a,h)anthracene*	0.011	0.016	0.174	0.055	0.005
benzo(ghi)perylene*	0.040	0.039	0.228	0.012	0.014
Sum PAH EPA 16*	11.2	13.5	15.9	8.4	4.5
Sum 7 PAHs	6.7	7.0	10.8	5.8	3.2

25% load				
0.1%S	0.1%S	0.5%S	2.5%S	Bio30
µg/Sm3	µg/Sm3	µg/Sm3	µg/Sm3	µg/Sm3
0.000	0.000	0.005	0.000	0.000
0.023	0.000	0.035	0.122	0.020
0.004	0.000	0.008	0.036	0.006
0.041	0.000	0.111	0.000	0.047
0.028	0.018	0.040	0.195	0.105
0.000	0.000	0.000	0.000	0.000
0.000	0.000	0.000	0.000	0.000
0.060	0.194	0.114	0.981	0.267
0.832	0.000	1.429	0.237	0.562
2.907	2.717	1.706	5.637	1.393
0.460	0.205	0.168	1.089	0.238
5.407	4.083	2.664	6.833	1.622
2.058	1.024	1.772	2.107	0.620
10.487	6.918	4.921	5.532	2.090
3.068	0.853	3.584	2.631	1.201
5.672	2.250	7.914	6.965	3.019
0.797	0.257	1.380	1.119	0.544
0.718	0.224	0.979	0.688	0.491
0.786	0.283	2.708	2.035	0.504
0.229	0.060	1.006	0.266	0.137
0.025	0.016	0.488	0.091	0.007
0.056	0.019	0.364	0.335	0.056
0.021	0.004	0.396	0.293	0.016
0.126	0.047	0.834	0.308	0.116
27.4	14.5	26.5	27.2	10.5
10.6	3.7	15.6	12.3	5.5

Table S6. On-board MSD engine in laboratory, Campaign B. Gaseous emissions, PM and its composition, BC (FSN-based), metals and PAHs.

Average concentrations (mass per Sm3 dry). ME1 after scrubber, ME2 after SCR and scrubber.

Component	Instrument	Unit	ME2	ME2	ME1	ME1
			75% load	40% load	75% load	40% load
NOx		g/Sm3 (dr	0.21	0.76	2.19	3.10
CO		g/Sm3 (dr	0.10	0.14	0.07	0.10
CO2		g/Sm3 (dr	114	98	119	104
O2 (dry)		vol%	12.8	14.2	12.9	13.7
H2O	FTIR	g/Sm3 (we	15.3	27.6	17.7	15.4
NO2	FTIR	mg/Sm3 d	1.2	4.2	50.1	133.6
CH4	FTIR	mg/Sm3 d	bd	bd	bd	bd
N2O	FTIR	mg/Sm3 d	bd	bd	bd	bd
NH3	FTIR	mg/Sm3 d	0.0	0.3	1.3	0.0
SO2	FTIR	mg/Sm3 d	1.1	2.1	6.3	3.0
Formaldeh	FTIR	mg/Sm3 d	bd	bd	bd	bd
Acetaldeh	FTIR	mg/Sm3 d	bd	bd	bd	bd
PM	ISO 8178 (mg/Sm3 d	21.7	16.9	29.9	38.1
BC	AVL 415SE	mg/Sm3 d	3.3	3.0	3.6	3.6
BC	AVL MSS	mg/Sm3 d	1.5	2.1	2.4	2.6
BC	MAAP	mg/Sm3 d	2.1	2.2	3.5	3.2
BC	AE33	mg/Sm3 d	2.9	2.5	4.0	4.5
EC (EUSAAP	PM: ISO81	mg/Sm3 d	1.4	1.5	1.9	2.1
PM: SO4		mg/Sm3 d	4.9	4.2	4.7	5.8
PM: NO3		mg/Sm3 d	0.0	0.1	0.1	0.1
PM: PO4, Br, Cl, F		mg/Sm3 d	0.8	0.2	0.4	0.4
PM: OC		mg/Sm3 d	7.3	4.5	13.5	16.4
PM: metals		mg/Sm3 d	3.4	2.2	2.1	3.5
PM: EC		mg/Sm3 d	1.4	1.5	1.9	2.1
Rest of PM		mg/Sm3 d	3.9	4.2	7.3	9.9
Ca		mg/Sm3 d	0.38	0.26	0.26	0.47
Fe		mg/Sm3 d	0.31	0.27	0.23	0.35
Mg		mg/Sm3 d	0.08	0.05	0.05	0.10
Mo		mg/Sm3 d	0.08	0.07	0.04	0.11
Na		mg/Sm3 d	0.40	0.36	0.23	0.46
Ni		mg/Sm3 d	0.27	0.20	0.25	0.28
P		mg/Sm3 d	0.01	0.01	0.01	0.02
V		mg/Sm3 d	0.38	0.28	0.41	0.43
benz(a)anthracene*		µg/Sm3 d	0.1	0.0	0.1	0.4
chrysene*		µg/Sm3 d	1.7	1.2	1.7	4.2
benzo(b)fluoranthene		µg/Sm3 d	0.3	0.2	0.3	0.8
benzo(k)fluoranthene		µg/Sm3 d	0.2	0.2	0.2	0.5
benzo(a)pyrene*		µg/Sm3 d	0.0	0.0	0.0	0.1
indeno(1,2,3-cd)pyrene		µg/Sm3 d	0.0	0.0	0.1	0.2
dibenz(a,h)anthracene		µg/Sm3 d	0.1	0.0	0.1	0.4
PAH6		µg/Sm3 d	2.3	1.7	2.6	6.5

* Before scrubber (ME1/HFO, ME1/MGO, ME2/HFO) and before SCR (ME2/HFO) in the Figures.

References

- Aakko-Saksa, P., Murtonen, T., Vesala, H., Koponen, P., Nyyssönen, S., Puustinen, H., Lehtoranta, K., Timonen, H., Teinilä, K., Hillamo, R., Karjalainen, P., Kuittinen, N., Simonen, P., Rönkkö, T., Keskinen, J., Saukko, E., Tutuianu, M., Fischerleitner, R., Pirjola, L., Brunila, O.-P. and Hämäläinen, E.: Black carbon measurements using different marine fuels, CIMAC Paper 068, 28th CIMAC World Congr., 2016.
- Aakko-Saksa, P., Murtonen, T., Vesala, H., Koponen, P., Timonen, H., Teinilä, K., Aurela, M., Karjalainen, P., Kuittinen, N., Puustinen, H., Piimäkorpi, P., Nyyssönen, S., Martikainen, J., Kuusisto, J. and Niinistö, M.: Black carbon emissions from a ship engine in laboratory (SEA-EFFECTS BC WP1), , 112, 2017.
- Aakko-Saksa, P. et al.: CIMAC Presentation 068 Black carbon measurements using different marine fuels, CIMAC Congr. 2016, 2016.
- Amanatidis, S., Ntziachristos, L., Karjalainen, P., Saukko, E., Simonen, P., Kuittinen, N., Aakko-Saksa, P., Timonen, H., Rönkkö, T. and Keskinen, J.: Comparative performance of a thermal denuder and a catalytic stripper in sampling laboratory and marine exhaust aerosols, *Aerosol Sci. Technol.*, 6826, 1–13, doi:10.1080/02786826.2017.1422236, 2018.
- Arnott, W. P., Hamasha, K., Moosmüller, H., Sheridan, P. J. and Ogren, J. A.: Towards aerosol light-absorption measurements with a 7-wavelength aethalometer: Evaluation with a photoacoustic instrument and 3-wavelength nephelometer, *Aerosol Sci. Technol.*, 39(1), 17–29, doi:10.1080/027868290901972, 2005.
- AVL List GmbH: Smoke Value Measurement With the Filter-Paper-Method. Application Notes. AT1007E, Rev. 03., 2014.
- Bond, T. C., Doherty, S. J., Fahey, D. W., Forster, P. M., Bernsten, T., Deangelo, B. J., Flanner, M. G., Ghan, S., Kärcher, B., Koch, D., Kinne, S., Kondo, Y., Quinn, P. K., Sarofim, M. C., Schultz, M. G., Schulz, M., Venkataraman, C., Zhang, H., Zhang, S., Bellouin, N., Guttikunda, S. K., Hopke, P. K., Jacobson, M. Z., Kaiser, J. W., Klimont, Z., Lohmann, U., Schwarz, J. P., Shindell, D., Storelvmo, T., Warren, S. G. and Zender, C. S.: Bounding the role of black carbon in the climate system: A scientific assessment, *J. Geophys. Res. Atmos.*, 118(11), 5380–5552, doi:10.1002/jgrd.50171, 2013.
- Collaud Coen, M., Weingartner, E., Apituley, A., Ceburnis, D. and Fierz-Schmidhauser, R.: Minimizing light absorption measurement artifacts of the Aethalometer: evaluation of five correction algorithms, *Atmos. Meas. Tech.*, 3, 457–474, doi:10.5194/amt-3-457-2010, 2010.
- Conrad, B. M. and Johnson, M. R.: Mass absorption cross-section of flare-generated black carbon: Variability, predictive model, and implications, *Carbon N. Y.*, 149, 760–771, doi:10.1016/j.carbon.2019.04.086, 2019.
- Cyrys, J., Heinrich, J., Hoek, G., Meliefste, K., Lewné, M., Gehring, U., Bellander, T., Fischer, P., Van Vliet, P., Brauer, M., Wichmann, H. E. and Brunekreef, B.: Comparison between different traffic-related particle indicators: Elemental carbon (EC), PM_{2.5} mass, and absorbance, *J. Expo. Anal. Environ. Epidemiol.*, 13(2), 134–143, doi:10.1038/sj.jea.7500262, 2003.
- Drinovec, L., Močnik, G., Zotter, P., Prévôt, A. S. H., Ruckstuhl, C., Coz, E., Rupakheti, M., Sciare, J., Müller, T., Wiedensohler, A. and Hansen, A. D. A.: The “dual-spot” Aethalometer: An improved measurement of aerosol black carbon with real-time loading compensation, *Atmos. Meas. Tech.*, 8(5), 1965–1979, doi:10.5194/amt-8-1965-2015, 2015.
- Hyvärinen, A. P., Vakkari, V., Laakso, L., Hooda, R. K., Sharma, V. P., Panwar, T. S., Beukes, J. P., Van Zyl, P. G., Josipovic, M., Garland, R. M., Andreae, M. O., Pöschl, U. and Petzold, A.: Correction for a measurement artifact of the Multi-Angle Absorption Photometer (MAAP) at high black carbon mass concentration levels, *Atmos. Meas. Tech.*, 6(1), 81–90, doi:10.5194/amt-6-81-2013, 2013.
- Keskinen, J. and Rönkkö, T.: Can real-world diesel exhaust particle size distribution be reproduced in the laboratory? A critical review, *J. Air Waste Manag. Assoc.*, 60(10), 1245–1255, doi:10.3155/1047-3289.60.10.1245, 2010.
- MAGEE: Aethalometer® Model AE33. User Manual., , (July), 1–52, 2015.
- McGill, R., Storey, J., Wagner, R., Irick, D., Aakko, P., Westerholm, M., Nylund, N.-O. and Lappi, M.: Emission Performance of Selected Biodiesel Fuels, *SAE Tech. Pap. Ser.*, 2003-01-18, 2003.
- Monica Tutuianu: AVL Technical Expertise on Black Carbon Measurement. Presentation in the ICCT 6th Workshop on Marine Black Carbon Emissions., ICCT, Helsinki., 2019.
- Petzold, A., Kramer, H. and Scöllner, M.: Continuous Measurement of Atmospheric Black Carbon Using a Multi-Angle Absorption Photometer, *Environ. Sci. Pollut. Res.*, 4, 78–82., 2002.
- Rönkkö, T., Virtanen, A., Vaaraslahti, K., Keskinen, J., Pirjola, L. and Lappi, M.: Effect of dilution conditions and driving parameters on nucleation mode particles in diesel exhaust: Laboratory and on-road study, *Atmos. Environ.*, 40(16), 2893–2901, doi:10.1016/j.atmosenv.2006.01.002, 2006.
- Schindler, W. and Singer, W.: Notes on "Soot" Measurement of Diesel Engines, n.d.
- Schindler, W., Haisch, C., Beck, H. A., Niessner, R., Jacob, E., Rothe, D., Schindler, W., Haisch, C., Beck, H. A., Niessner, R., Jacob, E. and Rothe, D.: A Photoacoustic Sensor System for Time Resol Quantification of Diesel Soot Emissions. Paper 2004-01-1968., *SAE Trans.*, 113, 483–490, 2004.
- Timonen, H., Aakko-Saksa, P., Kuittinen, N., Karjalainen, P., Murtonen, T., Lehtoranta, K., Vesala, H., Bloss, M., Saarikoski, S.,

Koponen, P., Piimäkorpi, P. and Rönkkö, T.: Black carbon measurement validation onboard (SEA- EFFECTS BC WP2). Report VTT-R-04493-17., 2017.

Zotter, P., Herich, H., Gysel, M., El-Haddad, I., Zhang, Y., Mocnik, G., Hüglin, C., Baltensperger, U., Szidat, S. and Prévôt, A. S. H.: Evaluation of the absorption Ångström exponents for traffic and wood burning in the Aethalometer-based source apportionment using radiocarbon measurements of ambient aerosol, *Atmos. Chem. Phys.*, 17(6), 4229–4249, doi:10.5194/acp-17-4229-2017, 2017.